frontiers in Natural Products

TYPE Original Research
PUBLISHED 12 August 2026
DOI 10.3389/fntpr.2026.1797194

Check for updates

OPEN ACCESS

EDITED BY
Imen Bouhaouel,
National Agronomic Institute of Tunisia (INAT)-Laboratory of Genetics and Cereal Breeding, Tunisia

REVIEWED BY
Neha Naaz,
Aligarh Muslim University, India
Tyson Tebogo Mokgalabone,
University of Limpopo, South Africa
Fabiola Eugelio,
Università degli studi di Teramo, Italy

*CORRESPONDENCE
Thomas Classen,
t.classen@fz-juelich.de

RECEIVED 27 January 2026
REVISED 20 May 2026
ACCEPTED 29 May 2026
PUBLISHED 12 August 2026

CITATION
Sowa P, Loehrer M, Gätgens J, Singh M, Beers A, Wiese-Klinkenberg A, Beier S, Noack S, Schaffrath U, Pietruszka J and Classen T (2026) Seed ripening and quinolizidine alkaloid dynamics in *Lupinus mutabilis*: from gene activity to metabolites.
Front. Nat. Prod. 5:1797194.
doi: 10.3389/fntpr.2026.1797194

COPYRIGHT
© 2026 Sowa, Loehrer, Gätgens, Singh, Beers, Wiese-Klinkenberg, Beier, Noack, Schaffrath, Pietruszka and Classen. This is an open-access article distributed under the terms of the Creative Commons Attribution License (CC BY). The use, distribution or reproduction in other forums is permitted, provided the original author(s) and the copyright owner(s) are credited and that the original publication in this journal is cited, in accordance with accepted academic practice. No use, distribution or reproduction is permitted which does not comply with these terms.

Seed ripening and quinolizidine alkaloid dynamics in *Lupinus mutabilis*: from gene activity to metabolites

Philipp Sowa[1,2], Marco Loehrer[2,3], Jochem Gätgens[2,4], Mansi Singh[2,5], Ashley Beers[1,2], Anika Wiese-Klinkenberg[2,5], Sebastian Beier[2,5], Stephan Noack[2,4], Ulrich Schaffrath[2,3], Jörg Pietruszka[1,2,6] and Thomas Classen[2,6]*

[1]Institute for Bioorganic Chemistry, Heinrich Heine University Duesseldorf, Juelich, Germany, [2]Bioeconomy Science Center (BioSC), Juelich, Germany, [3]Institute for Biology III, Department of Plant Physiology, RWTH Aachen University, Aachen, Germany, [4]Institute of Bio- and Geosciences 1: Biotechnology (IBG-1), Forschungszentrum Juelich GmbH, Juelich, Germany, [5]Institute of Bio- and Geosciences 4: Bioinformatics (IBG-4), Forschungszentrum Juelich GmbH, Juelich, Germany, [6]Institute of Bio- and Geosciences 1: Bioorganic Chemistry (IBG-1), Forschungszentrum Juelich GmbH, Juelich, Germany

Lupins are high-protein feed and food crops, but most species synthesize toxic quinolizidine alkaloids (QAs). Sweet lupins have been bred for low alkaloid levels, yet occasional reversion to the bitter, toxic phenotype requires routine monitoring for food safety. Understanding QA biosynthesis, transport, and seed accumulation is crucial for developing lupins as reliable crops and for strategies aimed at reducing toxicity or valorising alkaloids. Eight major QAs were quantified during seed ripening in *Lupinus angustifolius* and *L. mutabilis*. Pearson correlation analyses explored relationships among alkaloids and informed a hypothesis on pod-to-seed transport, especially in *L. mutabilis*. Semi-quantitative profiling of ten putative minor alkaloids complemented the study, and targeted transcriptomics measured expression of QA-biosynthetic and candidate transporter genes in pods and seeds. Both species showed distinct temporal accumulation patterns of the eight major QAs. Correlation data supported the hypothesis that pods are the primary QA source, with subsequent translocation to seeds in *L. mutabilis*. Minor-alkaloid profiling expanded the alkaloid spectrum. Transcriptomics revealed low QA-biosynthetic gene expression in seeds but detectable transporter gene expression, consistent with pod-derived QA import. The evidence indicates that QA synthesis occurs mainly in pods, followed by transporter-mediated movement into seeds. Recognising pods as the QA source provides a knowledge-based target for reducing seed toxicity or for exploiting alkaloid transport pathways in future lupin crop improvement.

KEYWORDS
alkaloid profile, bitter lupin, lupanine, quantification, sparteine, transcriptomics

1 Introduction

Lupin seeds are a protein source for animal and human nutrition (van de Noort, 2024). The high protein content rivals global crops like soybean while being rich in fiber and low in starch (Hove, 1974). In addition to exhibiting an increased resistance to climatic and biotic stress, lupins form a taproot system that improves soil structure. They are also able to fix atmospheric nitrogen via symbiotic interaction with rhizobia, thus mitigating soil nitrogen depletion (Pueyo et al., 2021). Agriculturally, bitter lupins, exhibiting a high quinolizidine alkaloid (QA) content toxic for mammals and humans alike, are discriminated from sweet lupins (Schrenk et al., 2019). On the one hand, sweet lupins are less harmful as food and feed; on the other hand, field cultures might suffer from increased susceptibility toward arthropod plant pests and herbivores (Talhinhas et al., 2016; Rodés-Bachs and Van der Fels-Klerx, 2023; Frick et al., 2018). Sweet lupins are a result of plant selection and breeding; however, there might be stress-induced titer increases and revertants bearing a high alkaloid content; thus, alkaloid monitoring is recommended in food affairs (Schrenk et al., 2019). The most widely accepted biosynthetic pathway for QAs (see Figure 1) has been proposed by Mancinotti et al. (202) and Schoofs et al. (1983), starting with the amino acid L-lysine (**1**). This is decarboxylated to form cadaverine (**2**) using a L-lysine decarboxylase (Schoofs et al., 1983).

Subsequently, cadaverine (**2**) is oxidized by a copper amine oxidase (CAO) to 5-aminopentanal (**3**), which cyclizes to Δ^1-piperideine (**4**) (Mancinotti et al., 2022). By tautomerism, Δ^1-piperideine (**4**) and Δ^2-piperideine (**5**) equilibrate. Both molecules may couple in an aldol-like reaction to (2′*R*,3′*R*)-tetrahydroanabasine (**6**) stereoselectively. The absence of enantiomers highlights the involvement of an enzyme. The natural compound **6** is the last analytically known compound of the following biosynthesis hypothesis. This hypothesis is illustrated in Figure 1. Although definite proof could not yet be provided, the most accepted hypothesis is the attachment of yet another Δ^1-piperideine subunit to provide the bisquinolizidine scaffold (**11**), which is the basis for all tri- and tetracyclic QAs (Mancinotti et al., 2022; Namdar et al., 2024). Neither the diiminium ion (**11**) nor its deprotonated states such as compound **12** have ever been detected. From there on, the reaction mechanism is almost completely unknown, with different hypotheses known in the literature: While some argue for separated derivatization of lupanine (**13**) and sparteine (**14**) with further modification toward hydroxylupanines and vinyl-side chains, others see sparteine (**14**) as the precursor alkaloid, which is decorated (Schoofs et al., 1983). Much of the older literature used *in vivo* radioactive labeling that was mostly unsuccessful, so a new approach was first tried by Namdar et al. (Namdar et al., 2024; Schütte and Hindorf, 1965; Golebiewski and Spenser, 1988; Rana and Robins, 1984). Using correlation-based analysis of different bitter lupin species, the phylogenetic analysis of the heritage of alkaloids was partly uncovered (Namdar et al., 2024).

A recent review on the chemodiversity of QA listed 397 individual compounds, of which more than 170 were lupin based (Cely-Veloza et al., 2023). They differ from each other in line, accession, variety, and environment, with some having pharmaceutical or ligand-type applications (Wrobleski and Long, 1977; Zeng et al., 2025; Villalpando-Vargas and Medina-Ceja, 2016). The biosynthesis of these toxins mainly takes place in the green organs of the plant, with a particular focus on the leaves (Frick et al., 2025; Lee et al., 2006). From the aerial epidermis, the alkaloids are

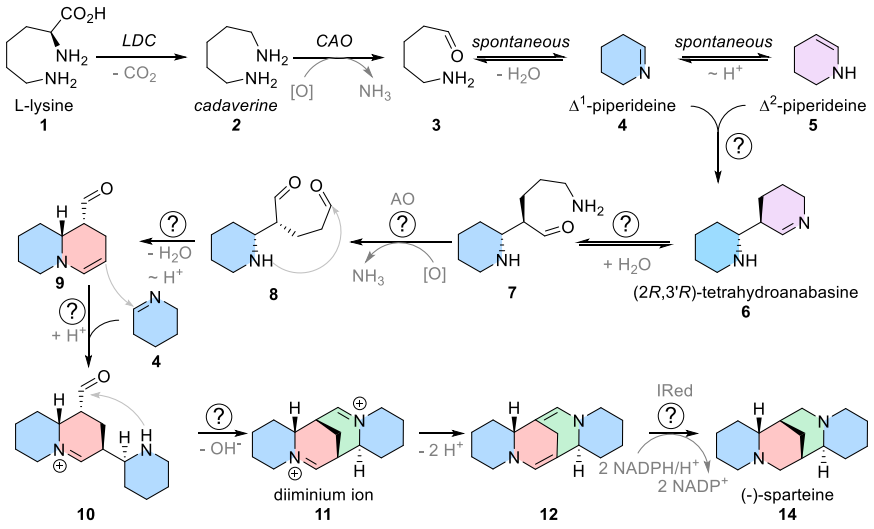


FIGURE 1
Proposed biosynthesis of the quinolizidine alkaloids (QAs) starting from L-lysine (**1**). The biosynthesis of Δ^1-piperideine (**4**) is known from other natural products, such as the biosynthesis of piperine (**6**). In addition, the aldol-like adduct (2*R*,3′*R*)-tetrahydroanabasine (**6**) could be analytically detected, although the putative enzyme responsible for this remains unknown. All other intermediates (**7–11**) are mechanistically plausible, but fully hypothetical. None of the enzymes responsible for these reactions are currently known. The current biosynthesis route is postulated to end with the diiminium ion (**11**), which has never been detected. This scheme shows the deprotonated compound **12** as a hypothetical intermediate for ion **11**. From this intermediate, the QAs found in lupins may be synthesized by oxidation or, for instance, reduction [e.g., sparteine (**14**)]. Reactions in which enzymes might be necessary have been marked with circled question marks. Abbreviations: LDC, lysine decarboxylase; CAO, copper amine oxidase; AO, amine oxidase; IRed, imine reductase.

TABLE 1 Overview of the aging stages 1–5. The stages used in this work have been correlated to a lupin development scale (Dracup and Kirby, 1996). Seeds and pods have been harvested and categorized according to this scheme. A phenomenological impression is shown in Figure 3.

Experimental stage	Harvest timing	Pod/seed characteristic	Development stage according to literature (Dracup and Kirby, 1996)
1	5–14 days post anthesis	Pods 1–3 cm; ovule primordia to small seeds	4.0
1.5	~20 days post anthesis	Pods 4.5–5 cm; pods/seeds green	4.1
2	60 days post stage 1	Pods 7–8.5 cm; green mature	5.4 to 5.5
3	>60 days	Pod walls yellowing; seeds losing green color; moisture declines	5.6
4	>60 days	Yellow mature stage to physiological maturity	5.7
5	>60 days	Full pod and seed maturity Complete drying ("pod shattering stage")	5.9

transported into the remaining plant parts, making the plant entirely toxic, with some of the alkaloids even being exported to the surrounding soil by the roots (Hama et al., 2022). This export was already investigated and led to the hypothesis that core alkaloids lupanine (**13**) and sparteine (**14**), as well as esterified lupanines, are transported via the phloem to their respective destination. Arriving at the seeds, the alkaloids are transmitted through the pods into the seeds, where they accumulate. Quite recently, this transfer was first investigated by Otterbach et al. (2019) in *L. angustifolius*.

The genes involved in these biosynthesis and transport processes have already been investigated by Bunsupa et al. (2012), leading to the functional confirmation of the genes encoding LDC and CAO. Loci like *iucundus* and *pauper* were linked to the sweetness or bitterness of seeds in *L. albus* (Frick et al., 2017). In *L. angustifolius,* an acetyltransferase (*LaAT*) possibly involved in acetylation in early QA biosynthesis from the *pauper* locus was identified, showing polymorphism causing sweetness in *L. angustifolius* (Mancinotti et al., 2023). The APETALA2/ethylene response transcription factor *RAP2-7* gene on the locus *iucundus* determines bitterness in *L. angustifolius* (Kroc et al., 2019). In addition to these results, identifying biosynthetic genes and transport mechanisms remains one of the biggest challenges in lupin research.

This study used the knowledge of different alkaloid profiles over the developmental stages. The hypothesis was that green tissues, especially in the young plants, are biosynthesizing QAs, which are then transported into reproductive organs where they accumulate and are also modified. Both the *L. mutabilis* and *L. angustifolius* [cv. Oskar; Otterbach et al. (2019) used as reference in this study] alkaloid time series were investigated. This sheds light on their major and minor QA relations and biosynthesis. In addition to analyzing the alkaloid content, the study analyzes transcriptomic data to correlate changes in alkaloid content with altered expression of genes involved in and related to QA biosynthesis and transport. For this, 33 gene homologs co-expressed with LDC first found by Yang et al. (2017), including a purine permease 1-like gene encoding a putative alkaloid transporter and a Myb-like transcription factor that might be involved in the regulation of QA biosynthesis, were investigated.

2 Materials and methods

2.1 Biochemical methods

2.1.1 Chemicals

All chemicals were purchased at Roth, Sigma-Aldrich, or TCI in the respective highest purity (at least 98%).

2.1.2 Cultivation of lupins

The bitter lupin line *L. angustifolius* Bo9027 was donated by Saatzucht Steinach GmbH & Co KG, Steinach, Germany. *L. mutabilis* PI 457964 was obtained from the National Plant Germplasm System, United States Department of Agriculture-Agricultural Research Service (GRIN-Global, https://npgsweb.ars-grin.gov/gringlobal/search) in 2019 (Byrne et al., 2018). For details of the cultivation, see Supplementary Material; in short: The lupins were cultivated in an ED73:Vermiculite substrate in a fully controlled growing chamber. Seeds and pods have been harvested and categorized according to Table 1.

2.1.3 Alkaloid isolation

The isolation of the major alkaloids was performed using a method published previously (Brooke et al., 1996). After grinding the dried seeds (50 g) in a GK 600 blender (Rotor Lips AG) for 13 min (7 min intensity 2 of 7, 6 min intensity 5 of 7), all seeds were ground finely (<1 mm fragment size). The extraction of the alkaloids was performed in a Soxhlet-based approach described by Brooke et al. (1996). A 150 mL Soxhlet containing 50 g of ground material in a 33 mm × 180 mm cellulose thimble was run for 72 h at 85 °C in 300 mL methanol. Afterward, the solvent was removed *in vacuo*, and the extracts were stored at 4 °C.

TABLE 2 Limit of blank (LOB) and limit of detection (LOD) of the eight major alkaloids represented (Armbruster and Pry, 2008).

Alkaloid	LOB (mg alkaloid)	LOD (mg alkaloid)
Lupanine (**13**)	0.064	0.064
Sparteine (**14**)	0.084	0.084
3β-Hydroxylupanine (**15**)	0.054	0.054
13α-Hydroxylupanine (**16**)	0.095	0.096
Tetrahydrorhombifoline (**17**)	0.032	0.032
Hydroxytetrahydrorhombifoline (**18**)	0.008	0.009
Angustifoline (**19**)	0.100	0.101
Isolupanine (**20**)	0.016	0.016

2.1.4 pH-based extraction

The extracts were dissolved in a succession of 3 × 20 mL *aqua demin.* All aqueous layers were combined and transferred into a 500 mL separating funnel. An adjustment to pH 1 was reached by using 700 µL 37% (m/m) HCl in water. An extraction took place with 3 × 120 mL of dichloromethane. After the second extraction, the interphase was disrupted by adding 20 mL brine. The organic layer was discarded. The aqueous layer was adjusted to pH 11 (1.2 mL 10 M NaOH). The alkaloids were extracted using 6 × 120 mL dichloromethane. The combined organic layers with pH 11 were dried *in vacuo* at 800 mbar and stored at −20 °C under a nitrogen atmosphere (approx. 500–1,000 mg).

2.1.5 Preparative, chromatographic isolation

In accordance with the literature, the isolation of QA was performed using varying solutions of methanol, dichloromethane, and ammonia in silica-60 column chromatography [(Brooke et al., 1996); for details, see SI]. The chromatographic separation from extract (see above) of *L. angustifolius* Bo9027 seeds (50 g) yielded lupanine (**13**), isolupanine (**20**), angustifoline (**19**), and 13α-hydroxylupanine (**16**) in purities >95% determined by qNMR (see Supplementary Material). From extracts of *L. mutabilis* PI 457964 seeds, lupanine (**13**), sparteine (**14**), 3β-hydroxylupanine (**15**), tetrahydrorhombifoline (**17**), and hydroxytetrahydrorhombifoline (**18**) have been isolated (purity >90% based on qNMR).

2.1.6 GC-based quantification

After isolation, calibration standards were performed using the previously obtained isolates. Their purity was determined using qNMR (see Supplementary Material). All standard samples were individually dissolved in methanol [using as an internal standard 50 µg/mL caffeine as done in literature, for example, Reinhard et al. (2006)] at concentrations ranging from 0 to 1.5 mg/mL. Additional measurements revealed the limit of blank (LOB) and limit of detection (LOD) for each alkaloid (see Table 2). Calibration curves have been recorded following every maintenance of the analytical device. Intra- and inter-day precision values have not been determined. Matrix effects of the samples have not been elucidated.

2.1.7 Alkaloid extraction

The extraction was performed following the protocol of Muzquiz et al. (1994), where 100 mg of freeze-dried material was disrupted for 3 min at 30 Hz in a *Retsch* swingmill MM 400. The powder was transferred to a 50 mL plastic reaction tube (Falcon), and 10 mL aqueous 0.5 M HCl was added. The mixture was vortexed for 15 s and then sonified in a bath for 20 min. Afterward, the solids were precipitated by centrifugation for 40 min at 14,000 × g. The supernatant was transferred, and the process repeated by adding another 10 mL 0.5 M HCl. The supernatants (20 mL) were adjusted to pH 11 (1.2 mL 10 M NaOH). At this point, the extract mixture was transferred onto an *Extrelut NT20* (*Merck, Darmstadt, Germany*) column. After 20 min incubation, the alkaloids were eluted by addition of 3 × 20 mL dichloromethane. The combined eluate was evaporated, and the extract was dissolved in 1.5 mL methanol (internal standard: 50 µg/mL caffeine). The sample was analyzed by GC-MS according to the method described (see Supplementary Material).

2.1.8 RNA extraction

RNA was extracted from four replicates of seeds and pods of *Lupinus mutabilis* PI 457964 collected in the year 2025 at developmental stages 1.5 and 2, harvested from the same plants used for QA quantification. Total RNA was extracted from plant tissues using the Qiagen RNeasy Plant Mini Kit (Qiagen, Germany), according to the manufacturer's instructions. To eliminate genomic DNA, RNA samples were treated with Baseline ZERO DNase (Biosearch Technologies, Germany, 5.7 µL buffer, 1.7 µL enzyme) and incubated at 37 °C for 30 min. After DNase treatment, volumes were adjusted to 100 µl with RNase-free water, followed by the addition of 350 µl lysis (RLT) buffer (Qiagen RNeasy Plant Mini Kit, Qiagen, Germany) and 250 µL 100% ethanol. The solution was transferred to RNeasy columns (Qiagen RNeasy Plant Mini Kit, Qiagen, Germany), centrifuged at 10,000 × g for 15 s, and washed twice with 500 µL RPE buffer (Qiagen RNeasy Plant Mini Kit, Qiagen, Germany) for 15 s and for 2 min at 10,000 × g. RNA was eluted in two sequential 25 µL aliquots with RNase-free water, each incubated 1 min at room temperature and centrifuged at 10,000 × g for 1 min, yielding 50 µL RNA. Samples were adjusted to equal volumes using RNase-free water and mixed with an equal volume of

chloroform, followed by thorough inversion and gentle shaking for 10 min. The mixtures were centrifuged at 10,000 × g for 10 min at room temperature, and the aqueous phase was carefully transferred to fresh 1.5 mL microcentrifuge tubes, avoiding the interphase. To the aqueous fraction, 0.15 volumes of 3 M sodium acetate (pH 6.4) and 3 volumes of 100% ethanol were added and mixed by inversion. Nucleic acids were precipitated by centrifugation at 14,500 × g for 20 min at 4 °C. The resulting pellet was washed with 70% ethanol (v/v) and centrifuged at 10,000 × g for 5 min. After the wash, the supernatant was discarded, and the pellet was air-dried prior to resuspension in RNase-free water. RNA concentration and purity were assessed spectrophotometrically prior to downstream applications. Only samples with an RNA integrity number (RIN) ≥ 7.0 as determined in a 2100 Bioanalyzer system (Agilent, United States) were retained for library preparation. High-quality RNA samples were submitted to Novogene (Munich, Germany), where sequencing libraries with mRNA enrichment through polyA capture were prepared and sequenced on the Illumina NovaSeq X platform to generate 150-bp paired-end reads.

2.2 Instrumental methods

2.2.1 GC-MS-based analyses of QA profiles

The GC-MS detection method applied in the detection of the QA-alkaloid profiles (2 min 120 °C, 30 min 120 °C–300 °C (6 °C/min), 2 min 300 °C) was done under constant flow (1.2 mL/min) using an MS transfer line temperature of 320 °C with a split of 20 ml/min. The ion source temperature was set to 230 °C, and a detection of 50–550 amu started 2.5 min after injection to protect the detector.

2.2.2 GC-ToF-MS-based identification of minor QAs

For the detection of minor alkaloids in *L. angustifolius* and *L. mutabilis*, a GC-ToF-MS-based method was applied (Paczia et al., 2012). The extraction was performed similarly to GC-MS quantification, but in the last step, the solution was dissolved in 10 mM phosphate buffer pH 6.8 to meet the requirements of the derivatization.

2.2.3 NIST-based analysis

Minor QAs were identified using the National Institute of Standards and Technology (NIST) database and the NIST-compliant internal database JuPoD (NIST, 2020). First, a detection of the isolated major alkaloids yielded their RI values. Based on the mother mass and the fragment patterns, peaks with similar appearances were searched in alkaloid profiles of all aging stages in both species of lupins. As these compounds were all represented under 2% of the total alkaloid amount in the alkaloid profile, the isolation of the compounds from the available sources was impossible, and identification was rather difficult. To ensure trustworthy representation of the findings, fingerprint-like fragments with exact masses, as determined by GC-ToF-MS, were identified. Based on this information, the alkaloids could be subdivided into lupanine type, sparteine type, and esterified lupanines. If the fragment patterns and RI values matched above an 800/1,000 similarity score with an alkaloid measured in the databases above on the same column, it was sorted to its fragment-based group. It must be acknowledged that distinguishing isomers is not possible with this method. After finishing the identification process, the presence of each compound was verified by calculating the quotient from the area of the QA in question divided by the area of the corresponding standard. This result was then normalized individually for each QA and displayed in a color-coded matrix.

2.2.4 Kovats index determination (RI value)

The RI values of the major and minor alkaloids were analyzed in comparison to a 50 mg/L C10-40 alkane standard purchased from Sigma-Aldrich (Art. No. 68281). After running the standard on the GC-MS and the GC-ToF-MS, the RI values of the major and minor alkaloids were calculated using the formula

$$RI_x = (RI_{alkane2} - RI_{alkane1}) \cdot \left(\frac{Rt_x - Rt_{alkane1}}{Rt_{alkane2} - Rt_{alkane1}} \right) + RI_{alkane1}$$

with $RI_{alkane}\,(C_{10+2n}H_{22+4n}, n = \{0; \ldots; 10\})$: $= 1000 + 200 \cdot n$

where RI is the retention time index, Rt′ is the netto retention time (detection start GC-ToF-MS ~ 1.5 min), Rt is the brutto retention time, x is component x, alkane1 is an early alkane, and alkane2 is a late alkane.

2.2.5 Bioinformatic analysis

For raw sequencing data (ENA accession ID: PRJEB104093), quality assessment of the reads was performed using FastQC v0.12 (Andrews, 2010), and Illumina adapter sequences were removed using Trimmomatic version 0.40 (Bolger et al., 2014; Beier et al., 2026) using the default parameters. Cleaned reads were then mapped to the *L. mutabilis* PI 457964 ("Cruickshanks") reference genome using Salmon v1.10.1 (https://git.nfdi4plants.org/usadellab/Lupinus_mutabilis_cruickshanks_Genome) with quasi-mapping-based transcript quantification using default parameters (Patro et al., 2017). The resulting count matrices were used for downstream differential gene expression analysis. Four biological replicates were used for each developmental stage/tissue. RNA sequencing generated an average of approximately 59 million reads per sample. Gene-level raw counts were imported into R (v4.5.2), and differential expression analysis was performed using the DESeq2 package (Love et al., 2014). Within the DESeq2 framework, counts were normalized to account for differences in library size using size-factor estimation. Differentially expressed genes were identified using a false discovery rate (FDR) < 0.05 and an absolute $\log_2$ fold change ($|\log_2 FC|$) ≥ 2 across four comparisons of contrasting tissues (pods vs. seeds) and developmental stages (stage 1.5 vs. stage 2). All sequences of genes involved in alkaloid production in *L. angustifolius* genome assembly version 2.0 (https://lupinexpress.org/) and *L. albus genome* version

1.0 (Genbank ID: GCA_009771035.1) were downloaded, and a BLASTp version 2.15.0 search was conducted against an *L. mutabilis* PI 457964 ("Cruickshanks") custom protein database using an e-value threshold of 1×10^{-5} (Altschul et al., 1990). To find homologs, multiple sequence alignments were performed using Clustal Omega (Sievers et al., 2011). Homologs in *L. mutabilis* PI 457964 were confirmed based on the presence of conserved domains, targeting signals for subcellular localization, the catalytic sites in the case of enzymes, and overall protein length.

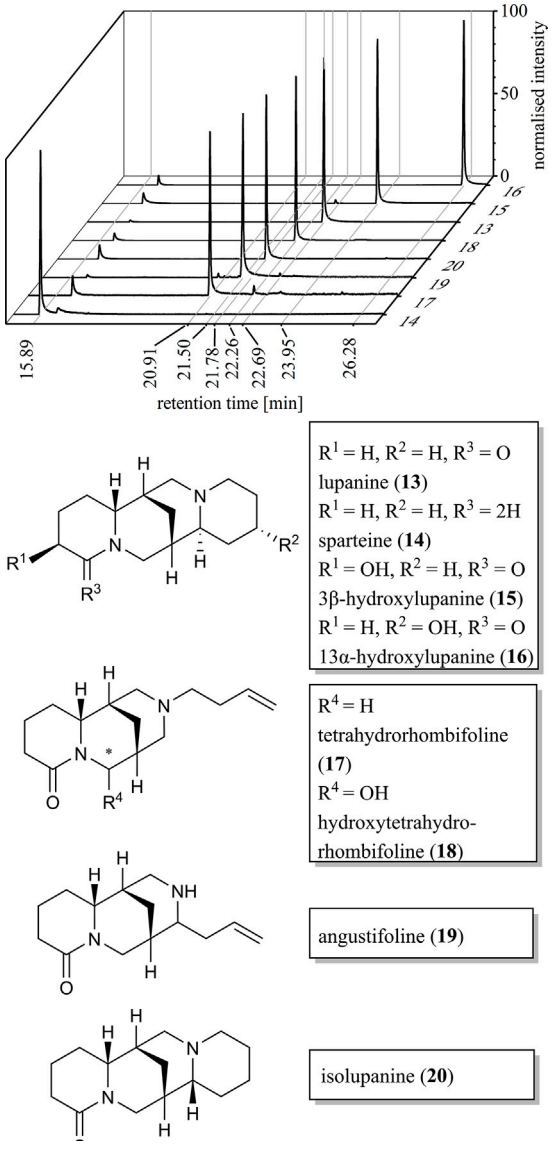


FIGURE 2
GC chromatograms of eight isolated major alkaloids present in *L. angustifolius* and *L. mutabilis* (normalized intensity 0–100) acquired by the isolation method described **(A)**. Identification of the alkaloids was performed by fragment analysis (for GC-ToF, RI values, and NMR results, see Supplementary Material). To enhance accuracy, caffeine (50 µg/mL in MeOH) was used as a standard. Major alkaloids are shown in subfigure **(B)**.

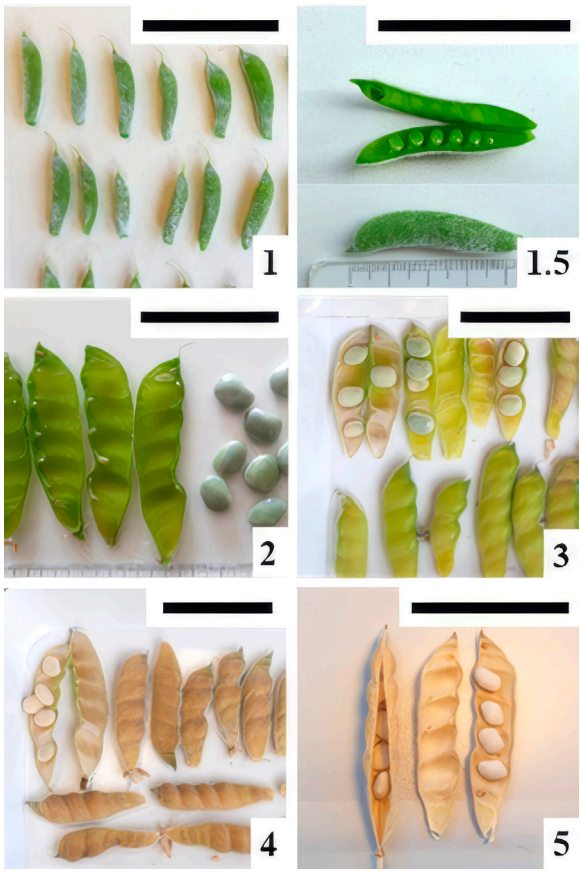


FIGURE 3
Exemplary images of the harvested *L. mutabilis* pod and seed development/ripening stages corresponding to the descriptions in the Material and Methods section. Stages are indicated by numbers in the lower right corners. Scale bars ≙ 5 cm.

3 Results

3.1 Establishing a GC-MS-based quantification method

The isolation of the major quinolizidine alkaloids (QA) in *L. angustifolius* Bo9027 and *L. mutabilis* PI 457964 was successfully performed (see Figure 2). The accuracy was tested using standard graphs of all eight major alkaloids, with the isolates gained from lupin seeds and caffeine as the standard. The quantification was established on a GC-ISQ-MS rather than the literature-established liquid chromatographic systems to combine major and minor alkaloid detection on one system.

3.2 QA quantification during the aging process

The quantification of the major alkaloids enabled the representation of *L. angustifolius* Bo9027 and *L. mutabilis* PI 457964 alkaloid profiles. During the generative phase, lupins can display all pod and seed aging stages simultaneously within a single plant, especially when considering branched and indeterminate varieties.

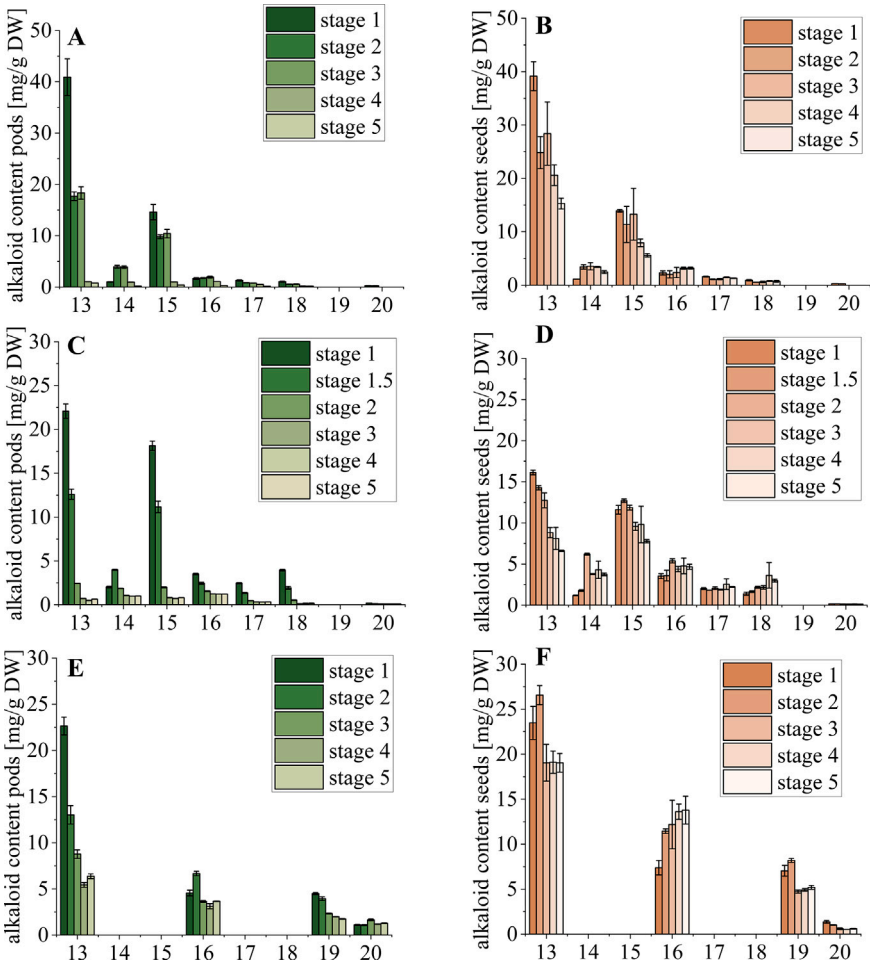


FIGURE 4
Major alkaloid contents during the aging process of *L. mutabilis* [**(A,B)** *anno* 2024, **(C,D)** *anno* 2025] and *L. angustifolius* [**(E,F)** *anno* 2024] seeds and pods. Displayed here are lupanine (13), sparteine (14), 3β-hydroxylupanine (15), 13α-hydroxylupanine (16), tetrahydrorhombifoline (17), hydroxytetrahydrorhombifoline (18), angustifoline (19), and isolupanine (20). Quantification of the major alkaloids in both species was performed using the GC-ISQ-MS-based quantification method described in Subsection 2.2.1 (mg/g DW). Error bars display deviations based on technical triplicates (N = 3); a larger representation of the graphs can be found in the Supplementary Material. Significance tests (p-value) were performed between adjacent stages investigating statistical significance (see Supplementary Table S4). According to the phenotypical aging steps, it could be shown that different alkaloids behave differently in seeds and pods depending on the alkaloid profile, aging step, and organ.

In other studies, the entire plant or specific parts were collected after fixed intervals, which might lead to an inhomogeneous pool of pods or seeds from different ripening stages. To overcome this limitation, here, phenotypical aging stages were used to guarantee harvest of biological samples from identical ripening stages and to facilitate a meaningful comparison between the two lupin species (for identification of the stages, see Table 1 and Figure 3). This also eliminates issues of varying ripening process speeds in seeds in different species and harvest generations. For better comparability, the alkaloid profiles were normalized to dry weight (mg/g dry weight (DW)). Seeds from 2024 of *L. angustifolius* have been used to compare the method with values obtained from the literature. In contrast, *L. mutabilis* was harvested for two consecutive years (2024, 2025), ensuring biological reproducibility of the results.

L. angustifolius had a less diverse major alkaloid profile than *L. mutabilis* and only four major alkaloids could be detected. These were lupanine (**13**), 13α-hydroxylupanine (**16**), angustifoline (**19**), and isolupanine (**20**). In the pods, lupanine (**13**) titers were reduced drastically in the early stages, while isolupanine (**20**) and 13α-hydroxylupanine (**16**) stayed mostly unaffected. A notable exception is stage 2, during which an increase in 13α-hydroxylupanine (**16**) was detected. Angustifoline (**19**) amounts also decreased in pods, while maintaining their content in seeds during development. In the seeds, the amount of lupanine remained the same. The experiments showed increased 13α-hydroxylupanine (**16**) and angustifoline (**19**) and decreased isolupanine (**20**) content over the course of the aging steps (see Figures 4E,F). The stagnation of lupanine is in accordance with previous studies (Otterbach et al., 2019). For comparison to Otterbach et al. (2019), the supporting information provides diagrams with alkaloid content per seed rather than dry weight (see Supplementary Figures 35–37). The profiles are similar in both studies for alkaloids lupanine (**13**) and 13α-hydroxylupanine (**16**) shared by Otterbach et al. (2019) and in this study.

For *L. mutabilis*, in addition to the alkaloids in *L. angustifolius*, sparteine (**14**), 3β-hydroxylupanine (**15**), tetrahydrorhombifoline

TABLE 3 *L. mutabilis* minor alkaloid analysis. The minor alkaloids were analyzed, and the results were subdivided into the relative abundance ($I_{alkaloid}$ [μVmin]/$I_{caffeine}$ [μVmin]). These values were normalized (0; 100) for each replicate separately. The averages of the normalized values are displayed with their standard deviation. The compounds are based on their MS-fragmentation pattern: sparteine-type (27, 28, 29), lupanine-type (24, 25, 26), hydroxylupanine-type (22), along with angustifoline-type (30) and an unidentified, esterified lupanine (21). The confidence limit of the typization was a similarity index score of >800/1,000 for the fragment pattern as calculated by NIST compared to the name-giving major alkaloid (National Institute of Standards and Technology, 2023). For the entire table with the relative abundances, see Supplementary Table S5. The results serve as the basis for Figure 8. Standard deviations are based on technical replicates (N = 3).

	Compound									
Stage ●seed ◇pod	21	22	23	24	25	26	27	28	29	30
●1	76 ± 23	0 ± 0	7 ± 12	0 ± 0	100 ± 0	100 ± 0	0 ± 0	0 ± 0	0 ± 0	0 ± 0
●1.5	78 ± 38	49 ± 45	55 ± 42	5 ± 1	49 ± 12	32 ± 4	0 ± 1	7 ± 10	10 ± 3	19 ± 17
●2	4 ± 1	72 ± 23	100 ± 0	100 ± 0	16 ± 2	12 ± 4	68 ± 17	100 ± 0	100 ± 0	34 ± 16
●3	0 ± 0	50 ± 31	41 ± 23	15 ± 8	7 ± 7	6 ± 4	58 ± 13	24 ± 7	41 ± 2	84 ± 28
●4	0 ± 0	91 ± 8	24 ± 29	33 ± 13	2 ± 2	8 ± 5	100 ± 0	33 ± 22	54 ± 17	75 ± 38
●5	0 ± 0	87 ± 20	10 ± 7	12 ± 7	3 ± 5	0 ± 0	61 ± 32	22 ± 14	34 ± 6	49 ± 20
◊1	100 ± 0	100 ± 0	100 ± 0	13 ± 4	100 ± 0	100 ± 0	34 ± 5	21 ± 10	25 ± 1	100 ± 0
◊1.5	69 ± 1	44 ± 3	37 ± 2	100 ± 0	32 ± 4	30 ± 9	100 ± 0	100 ± 0	100 ± 0	43 ± 4
◊2	2 ± 0	11 ± 3	10 ± 3	10 ± 3	3 ± 0	1 ± 0	77 ± 0	21 ± 8	11 ± 2	12 ± 0
◊3	0 ± 0	0 ± 0	1 ± 1	1 ± 1	0 ± 0	0 ± 0	9 ± 0	13 ± 2	0 ± 0	0 ± 0
◊4	0 ± 0	0 ± 0	1 ± 1	2 ± 0	0 ± 0	0 ± 0	1 ± 2	8 ± 7	1 ± 1	0 ± 0
◊5	0 ± 0	0 ± 1	0 ± 0	0 ± 1	1 ± 0	1 ± 1	2 ± 2	2 ± 3	0 ± 0	1 ± 2

(**17**), and hydroxytetrahydrorhombifoline (**18**) were detected, while angustifoline (**19**) was undetectable. The early stages have very similar alkaloid profiles for both seeds and pods (see Figures 4A–D). Lupanine (**13**) and its hydroxylated forms 3β-hydroxylupanine (**15**) and 13α-hydroxylupanine (**16**) were the main components of the early stages of the ripening process. During the growth of the seed in stages 2–3, the content of lupanine (**13**) reduced in both pods and seeds, while 13α-hydroxylupanine (**16**) appeared to be unaffected. With this reduction in lupanine (**13**) and lupanine derivatives, the amount of sparteine (**14**) increased and reached its maximum content in stages 2–3. Tetrahydrorhombifoline (**17**) and hydroxytetrahydrorhombifoline (**18**) were rather unaffected during the entire ripening process in seeds but showed reduced content in pods. In stage 3, the maximum weight of the seeds is reached, while the pods started decoloring (see Figure 3). During the drying stages 4–5, the pod alkaloid profile started to differ vastly from the seed alkaloid contents. Lupanine (**13**) and 3β-hydroxylupanine (**15**) were reduced in the seeds, and sparteine (**14**) remained constant. The alkaloid content of the pods was diminished in stage 5. The detection in both years (2024, 2025) for *L. mutabilis* displayed biological variation in the absolute alkaloid content, but the development of the alkaloid profiles over the course of the aging stages showed reproducible trends in both years. Thus, in the later analyses, these data were combined.

3.3 Minor QA analysis

The minor alkaloid analysis was performed using the library provided in SI on the basis of NIST20 (NIST, 2020). The data were acquired based on alkaloid profiles measured by GC-ISQ-MS, whilst exact m/z-ratios were obtained by GC-ToF-MS. In total, 24 putative alkaloids could be identified from the NIST dataset according to exact masses and RI values, respectively. Although an examination of all distinguishable peaks was performed, the library available in the SI might not represent every alkaloid present in *L. mutabilis* and *L. angustifolius* and does not distinguish between isomers. Ten putative alkaloids (**21**–**30**) were detectable in *L. mutabilis* by GC-ISQ-MS throughout all aging samples (see Table 3). These were clustered by comparison with the NIST database, which gave the most probable QA-type (NIST, 2020). Because no response factor for quantification is available for all these entities, further analyses must be considered semi-quantitative. The obtained data can be found in the Supplementary Table S5. In Figure 8, the normalized abundances have been joined based on the profile similarity. Foremost, data obtained from pods and seeds cluster per tissue except in the case of compounds **21, 25**, and **26**. Thus, it can be concluded that there are physiological differences between pods and seeds. Furthermore, it is clear that putative minor alkaloids obtained from pods are more abundant in the early stages (1–1.5), whereas seeds contain more of these compounds in the medium (2) or late (3–5) stages of ripening. The esterified, lupanine-type QAs (**21**) as well as the compounds **25** and **26** resemble the same pattern with a strong abundance in the early stages (<2).

3.4 Differential gene expression across tissues and developmental stages

After detection of alkaloid titers, transcriptomics was utilized to further investigate their biosynthetic origin. To gain insight into

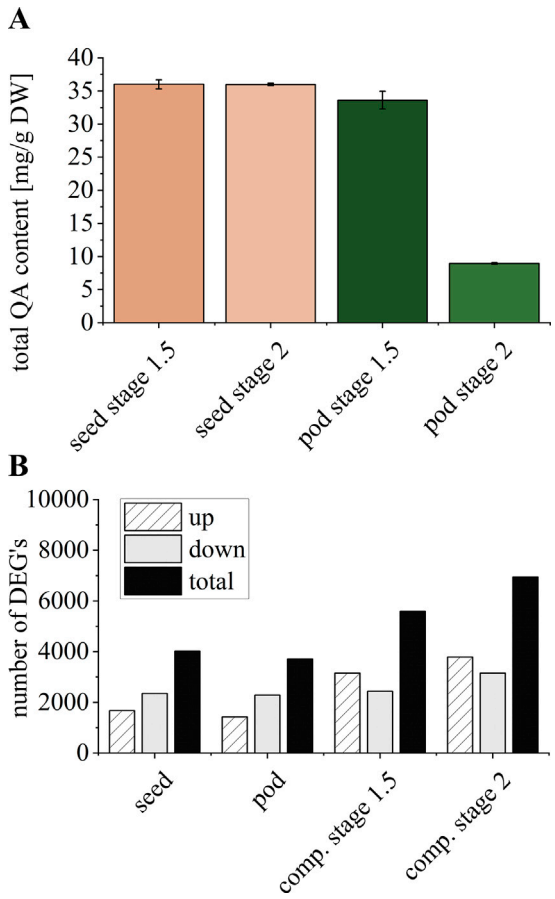


FIGURE 5
QA content and differential gene expression in stages 1.5 and 2 in pods and seeds. **(A)** Total major QAs at the investigated stages 1.5 and 2, average values of the sum of major alkaloids, three technical replicates (*anno* 2025). Error bars show standard deviation. **(B)** Comparison of up- and downregulated differentially expressed genes (DEGs) across different tissues and developmental stages. Genes selected with $\log_2$ fold changes of expression and with significant change of $p < 0.05$. Seed and pod = comparison stage 2 over stage 1.5. Comp. stage = comparison between pod and seed at stages 1.5 and 2.

transcriptional regulation during early pod and seed development in *L. mutabilis* PI 457964, mRNA sequencing was performed. As illustrated in Figures 4, 5A; Table 3, seeds and pods at stages 1.5 and 2 exhibited varying concentrations of major and minor QAs. These two stages were intentionally selected for two reasons: (a) it was assumed that both stages are highly active in terms of biosynthesis, and (b) they exhibit different alkaloid profiles. A principal component analysis was performed, showing clear clustering of the four replicates and separation by stage and tissue, reinforcing their phenotypical selection (see Supplementary Figure 47). Overall, 93% of the variance was explained by two principal components. At stage 2, seeds were more strongly separated from pods than at the earlier stage 1.5. Differential gene expression was analyzed in four comparisons, contrasting tissues (pods and seeds) and developmental stages (stage 1.5 and stage 2). Differentially expressed genes (DEGs) were defined as those with significant differences in expression levels between sample groups, based on FDR <0.05 and $|\log_2 FC| \geq 2$. The results revealed 3,708 DEGs in pods (see Supplementary Table S1, sheet 3) and 4,027 DEGs in seeds (see Supplementary Table S1, sheet 2) comparing the two stages (see Figure 5B). Tissue-specific differences were more pronounced, with 5,587 DEGs differentiating pods and seeds at stage 1.5 (see Supplementary Table S1, sheet 4), and 6,946 DEGs at stage 2 (see Supplementary Table S1, sheet 5; Figure 5B). A Pearson's correlation between quantified gene expression (transcripts per million, TPM) and QA concentrations resulted in large numbers of genes with high and significant correlations. With current knowledge, the possible candidates were too numerous to analyze. This necessitates further investigations into known components of the QA biosynthesis pathway. Pearson's correlation coefficient results are presented only for the DEGs (see Supplementary Table S1, sheets 2–5). In addition, Pearson's correlation coefficients for notable transcription factors (see Supplementary Table S1, sheets 6–9) and transporters (see Supplementary Table S1, sheets 10–13) associated with stage- and tissue-specific differences were also provided.

Therefore, 33 genes (see Supplementary Table S1, sheet 1) known to be involved in biosynthesis, transport, and regulation of quinolizidine alkaloids were specifically investigated, identified through homology with *L. angustifolius* and *L. albus* as outlined in Subsection 3.2.5 (Yang et al., 2017). The genes responsible for the initial enzymatic steps in QA biosynthesis, lysine decarboxylase (*LDC*) and copper amine oxidase (*CAO*), did not show statistically significant changes over time within either tissue (from stages 1.5–2). However, the *LDC* and *CAO* genes mikado.chr19G51 (homolog 1) and mikado.chr19G1289 (homolog 1) displayed strong tissue-specific enrichment in pods compared to seeds. They were upregulated in pods with $\log_2$ fold change values of ~8–9 at stage 1.5 and ~16–18 at stage 2 (see Supplementary Table S1, sheet 1). Similarly, cinnamoyl-CoA reductase 2 genes (*CCR2*), involved in plant secondary metabolism, present comparably increased expression in pods. Two acetyltransferase (*AT*) genes, homologous to *LaAT*, exhibited strong pod-enriched expression in stage 1.5 and reduction of expression in seeds and pods with development from stage 1.5 to stage 2 (see Supplementary Table S1, sheet 1). The 13-hydroxylupanine O-tigloyltransferase (*HMT/HLT*) gene mikado.chr5G47 was enriched in pods, also showing some increased expression in seeds in stage 2 compared to stage 1.5. In contrast, 4-hydroxy-tetrahydrodipicolinate synthase (*DHDPS*) genes, encoding a central enzyme in the primary lysine biosynthesis pathway, showed variable regulation that did not align with the expression patterns of specific QA-biosynthetic genes (*LDC/CAO*) (Kroc et al., 2019).

Putative transporter genes associated with the QA pathway, specifically purine permease 1 [*PUP1* (Hildreth et al., 2011; Plewiński et al., 2019; Martinez-Hernandez et al., 2025)] homologs mikado.chr12G757, mikado.chr12G1284, mikado.chr19G396, and mikado.chr2G1111 were significantly more abundant in pods than in seeds, with fold changes exceeding $\log_2 FC$ from 6 to 11 at both stages. *PUP1* genes also showed a reduction in expression with the development of the seeds and pods in stage 2. Regulatory candidates followed a similar trend as LCD and CAO; the *AP2/ERF* transcription factor *RAP2-7* and the transcription factor *MYB106* were consistently enriched in pod tissue with $\log_2 FC$ changes from 6 to 8.

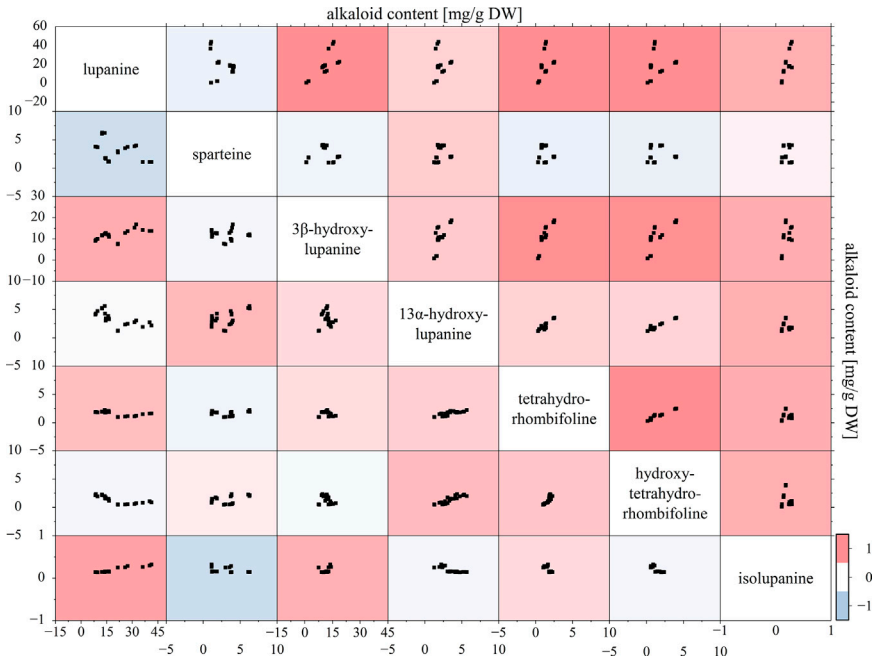


FIGURE 6
Correlation matrix of the major *L. mutabilis* alkaloids for stages 1–3. The correlation of the major alkaloids from *L. mutabilis* stage 1–3 seeds (lower left below the diagonal) and pods (upper right above the diagonal) is depicted here by using the Pearson correlation coefficient. This experiment was set up using the data of the biological replicates of 2024 and 2025 and is depicted by a scatter matrix. Each dot represents the measured alkaloid contents (mg/g DW) of two alkaloids in a single measurement represented in each box on the x-axis and y-axis, respectively. As the years differed in absolute alkaloid values (see Supplementary Figure 44), the correlations were averaged and represented by blue (negative correlation) and red (positive correlation), respectively. For better representation, the dataset is split into the two ripening phases, growth and drying (see Figure 7). Each box is based on biological replicates (N = 2) (2024, 2025) with separate technical replicates (N = 3). The correlation analyses were conducted on the entire dataset. The results showed that independent of the organ, some alkaloids correlate more than others.

4 Discussion

The investigation of pod and seed maturation in *L. mutabilis* was performed using the major QA titers, the qualitative content of the ten minor QAs, and a gene expression study. Previous studies, such as Otterbach et al. (2019), established a pod-to-seed QA transport hypothesis for *L. angustifolius*, and Namdar et al. (2024) recently revisited QA biosynthesis in wild lupin species. This work extends the understanding by adding species coverage with *L. mutabilis*, investigating seed and pod tissue throughout seed development and ripening, integrating transcriptomics and data from two growing seasons. In general, the absolute content of QA varies between stages, organs, and experimental biological repetitions. The difference in seeds compared to pods increases during the aging process, verifying the role as storage tissue. The pods reduce their alkaloid content during ripening with distinct differences between the green phenotypical stages 1–3 and stages 4–5, correlating with their decrease in chlorophyll and water content (see Figures 3, 4). The same phenotypical subclassification can be attributed to the seeds. Although alkaloid titer variance is persistent until stage 5, the major accumulation can be attributed to stages 1–3, with green and putative photosynthetically active seeds (see Figure 3). This suggests the hypothesis that either transport phenomena between the organs or the biochemical transformation of the alkaloids are causally related. One effect is also evident in a rough examination of the alkaloid profiles; for example, in *L. mutabilis,* the earlier stages within the pods show lupanine (**13**) and 3β-hydroxylupanine (**15**), while the older stages contain reduced amounts (see Figures 4B,D). For this reason, the data from stages 1–3 were pooled, and the data from stages 4 and 5 were combined. Pearson's correlation analyses were performed for all pairs of alkaloid contents within the respective data pools. This was done for pods and seeds separately, with seeds represented in the lower left part, while correlations in pods were placed in the upper right part of the graphs (see Figures 6, 7). These datasets include the technical replicates (N = 3) and also the biological replicates from both growing years. The results are represented in Figure 6 (age groups 1–3) and Figure 7 (age groups 4 and 5). The same analysis was done for the samples of *L. angustifolius* for the available data of 2024 solely (supplied in the Supplementary Figures 45,46).

The correlations of the alkaloids differed between both phases in *L. angustifolius* and *L. mutabilis* (see Figures 6, 7; Supplementary Figure 45,46). In stages 1–3, *L. angustifolius*, lupanine (**13**) correlates positively with angustifoline (**19**) in pods and seeds. In both organs, 13α-hydroxylupanine (**16**) correlates positively with lupanine only in stages 4–5, while no correlation between the alkaloids can be detected during the growing stages. The correlation between 13α-hydroxylupanine (**16**) and angustifoline (**19**) changes from positive to negative in the pods, while it changes from negative to positive in seeds (see Supplementary Figures 45,46). In contrast, isolupanine (**20**) correlates negatively with all other alkaloids in early pod stages, while positive correlations with its epimer (**13**) and angustifoline (**19**) can be seen in early seeds. The correlation with 13α-

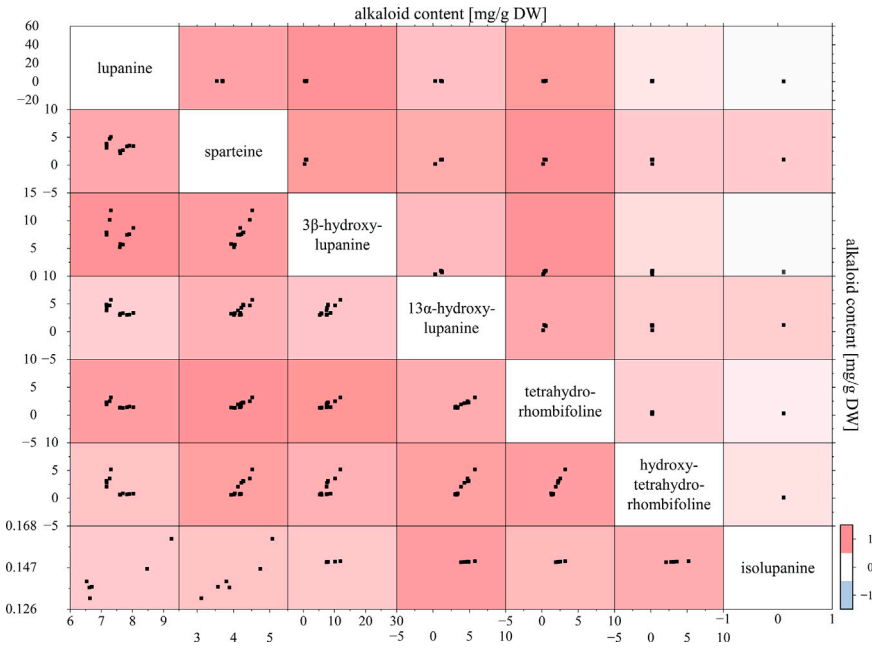


FIGURE 7
Correlation matrix of the major *L. mutabilis* alkaloids for the ripened stages 4–5. The correlation of the major alkaloids from *L. mutabilis* stages 4–5 seeds (lower left below the diagonal) and pods (upper right above the diagonal) is depicted here using the Pearson correlation coefficient. This experiment was set up using the data of the biological replicates of 2024 and 2025 and is depicted by a scatter matrix. Each dot represents the measured alkaloid contents [mg/g DW] of two alkaloids in a single measurement, represented in each box on the x-axis and y-axis, respectively. As the years differed in absolute alkaloid values (see Supplementary Figure 44), the correlations were averaged and represented by blue (negative correlation) and red (positive correlation), respectively. For better representation, the dataset is split into the two ripening phases, growth (see Figure 6) and drying. Each box is based on biological replicates (N = 2) (2024, 2025) with separate technical replicates (N = 3). The correlation analyses were conducted on the entire dataset. The results showed that independent of the organ, some alkaloids correlate more than others.

hydroxylupanine (**16**) changes from negative to positive in seeds over development (see Supplementary Figure 46). The data hint at stronger transport processes taking place into seeds in later stages, while negative correlations in earlier stages might indicate derivatization in seeds and pods alike. This is coherent with Otterbach et al. (2019), as they also describe accumulation of high titers of lupanine throughout the pod-seed complex maturation. A direct comparison to the previously published result is shown in Supplementary Figures S3, S7. As expected, there are differences in the analyzed alkaloid profile of the two investigated species. For example, angustifoline (**19**) is found exclusively in *L. angustifolius*, while sparteine (**14**), 3β-hydroxylupanine (**15**), tetrahydrorhombifoline (**17**) and hydroxytetrahydrorhombifoline (**18**) are found exclusively in *L. mutabilis*. The diversity of alkaloids presented here reveals a greater decrease in lupanine during the ripening process than is observed in *L. angustifolius*.

Lupinus mutabilis has the more complex major alkaloid profile. However, the correlation of almost all alkaloids was positive or very minor throughout both ripening stages, with the exception of lupanine (**13**), which had negative correlations in both lupin species. The alkaloid values of the most important alkaloids in stage 1.5 are identical in both the pods and the seeds, suggesting that the seeds and pods originate from a common precursor organ (see Figures 4A–D). The major alkaloids present early in development are lupanine (**13**) and 3β-hydroxylupanine (**15**). Starting the ripening process, the relation between lupanine (**13**) and sparteine (**14**) is negative in pods and seeds during their biosynthetic activity in both years (see Figure 6). This might suggest a precursor hypothesis. Isolupanine (**20**) has the lowest content of all major alkaloids. It correlates positively the strongest with lupanine (**13**) and negatively with sparteine (**14**) in stages 1–3, leading to the hypothesis that the same enzyme might be responsible for both. This putative enzyme might not be stereoselective toward these diastereomers. This enzyme would be downregulated later, explaining the late sparteine (**14**) accumulation in both pods and seeds alike. The hydroxylation of lupanine (**13**) through a putative monooxygenase might lead to 3β-hydroxylupanine (**15**) and 13α-hydroxylupanine (**16**). There must be an additional source, such as transport, because lupanine (**13**), 3β-hydroxylupanine (**15**), and 13α-hydroxylupanine (**16**) show a very strong positive correlation, which is in accordance with the transport hypothesis posed by earlier research (Lee et al., 2006; Otterbach et al., 2019).

An additional explanation for this phenomenon might be that esterified lupanines (**21**), which are present at the beginning of the seed ripening process according to Figure 8, might hydrolyze to form the hydroxyl group. Tetrahydrorhombifoline (**17**) and hydroxytetrahydrorhombifoline (**18**) accumulate in seeds, although with small titers compared to the other alkaloids. It cannot be distinguished whether these compounds are produced selectively or as a side product from promiscuous (oxidative) enzymes. Being an artifact of the extraction can be ruled out,

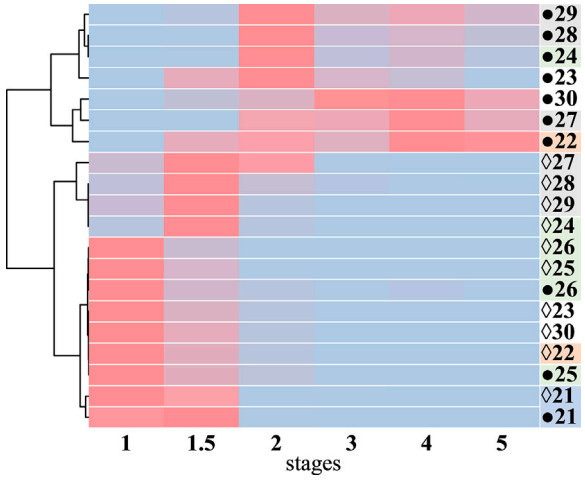


FIGURE 8
The minor alkaloid (MA) analysis of *L. mutabilis* (anno 2025) of seed (●) and pod (◊) using relative quantification via GC-MS. Minor alkaloids were detected according to their RI value and fragment pattern (the library is available from the repository associated with this publication). The data were normalized between the minimum and maximum measured peak integral at 0% (blue) and 100% (red) for each alkaloid. The compounds are based on their MS-fragmentation pattern: sparteine-type (gray, **27**, **28**, **29**), lupanine-type (green, **24**, **25**, **26**), and hydroxylupanine-type (orange, **22**), along with angustifoline-type (**30**) and an unidentified, esterified lupanine (blue, **21**). The confidence limit of the typization was a similarity index score of >800/1,000 to the major alkaloid fragment pattern, with the highest similarity as calculated by NIST compared to the name-giving major alkaloid. Details on Kovats indices (RI), m/z, and the putative molecular formula can be found in Supplementary Table S8. Each box is based on technical replicates (N = 3). The data have been clustered according to their quadratic Euclidean distances.

because these compounds did not occur in extractions of *L. angustifolius* (see Supplementary Figure 45,46). In stages 4–5, the reliance on import rather than local biosynthesis becomes apparent. As the alkaloid content in the pods reaches its minimum, all alkaloids correlate positively, which is in accordance with the published hypothesis of storage and drying (water loss, color changes, no bioactivity) (Otterbach et al., 2019). This also applied to *L. mutabilis*, for which bioactivity must have been decreased severely in stages 4–5, as it is monitored by the positive correlations of all alkaloid titers.

As is usual with secondary metabolisms, the late-stage derivatization of compounds is diversified to combat different threats (Firn and Jones, 2003). Based on this hypothesis, lupin alkaloid profiles should consist of some major and many minor alkaloids representing less than 2% of the total alkaloid content. Applying a library of compounds with exact masses gained from GC-ToF-MS measurements (the library is supplied in a repository; https://doi.org/10.26165/JUELICH-DATA/XNAIFH), a typification of the presenting minor compounds was performed (see Supplementary Table S8). Using the fragment patterns of GC-ISQ-MS (see Supplementary Figures 48–57), the compounds were clustered by their quadratic Euclidean distances, pairing similar appearances (see Figure 8). Generally, the data from pods and seeds clustered together, indicating their similarity to the same alkaloids generally appearing in the pods first. Esterified lupanines (**21**) are an exception to this rule. In the literature, it is hypothesized that esterified lupanines (**21**) are the transport form of QAs (Lee et al., 2006). This correlation suggests that their transport mechanism is direct, without other locations, or that the biosynthesis of esterified QAs occurs simultaneously in both organs in the early stages. This is supported by the fact that both organs are photosynthetically active at this point. Furthermore, a cluster of each lupanine- (**24**–**26**) and sparteine-type (**27**–**29**) can be observed in the pods. While lupanine-type (**24**–**26**) alkaloids appear rather early, sparteine-type alkaloids appear later, supporting the postulated derivatization of sparteines to lupanines by enzymatic derivatization. However, where the derivatization takes place is not known, as both types appear to transfer from pods to seeds. The hydroxylated product (**22**) appears in pods first and slowly accumulates in the seeds.

As deduced from experiments presented in this work and previous studies, a biosynthetic pathway hypothesis was postulated (see Figure 9).

As both lupanine (**13**) and isolupanine (**20**) exist, the ring-closure mechanism proposed in the literature may lead to a predetermination toward either lupanine (**13**) or its epimer (**20**). The negative correlation of lupanine (**13**) and sparteine (**14**), as well as structural advantages, leads to sparteine (**14**) as a precursor accumulating after the responsible monooxygenase is downregulated. The product lupanine is then either hydroxylated or the available esterified lupanines are hydrolyzed to enable an accumulation of hydroxylupanines (**15**, **16**). Additionally, transport mechanisms from pods to seeds increase the titer in the latter tissue, as is also suggested by the transcriptome analyses, while an additional import from other green plant organs is likely. From the hydroxylated QA in the 13-position (**16**), a ring opening is likely leading to tetrahydrorhombifoline (**17**) and hydroxytetrahydrorhombifoline (**18**). As the correlation analysis does not highlight a common temporal envelope, shared transcriptional regulation, or dilution by biomass accumulation separately, these factors could also be responsible for parts of the correlation drifts.

A gene expression study was conducted to further validate the results. Comparison of transcriptomes of seeds and pods at stage 1.5 and 2 reveals extensive changes due to tissue and development. This provided indications for the putative transport mechanisms hypothesized in Figure 9. The expression of key candidate genes is summarized in Figure 10 and visualized as transcripts per million values (TPM). Their differential expression profiles are provided in Supplementary Table S1, sheet 1.

The differential gene expression profiles of the identified QA biosynthesis-related genes indicated a difference in biosynthetic activity in seeds compared to pods. The substantial enrichment of *LDC* and *CAO* transcripts in pods relative to seeds, which is a phenomenon observed across the investigated developmental stages, identified the pod as the predominant biosynthetic "source" for the QAs even in early stages. This indicated scaffold building in the pods, which could then transfer either sparteine or lupanine as precursor molecules. These might then be derivatized in all green tissue (seeds and pods). This pattern was also congruent with *Lupinus angustifolius,* in which *LDC* expression peaks early in pods and was very low in developing seeds, while QA contents accumulated later in seeds (Otterbach et al., 2019; Frick et al., 2025).

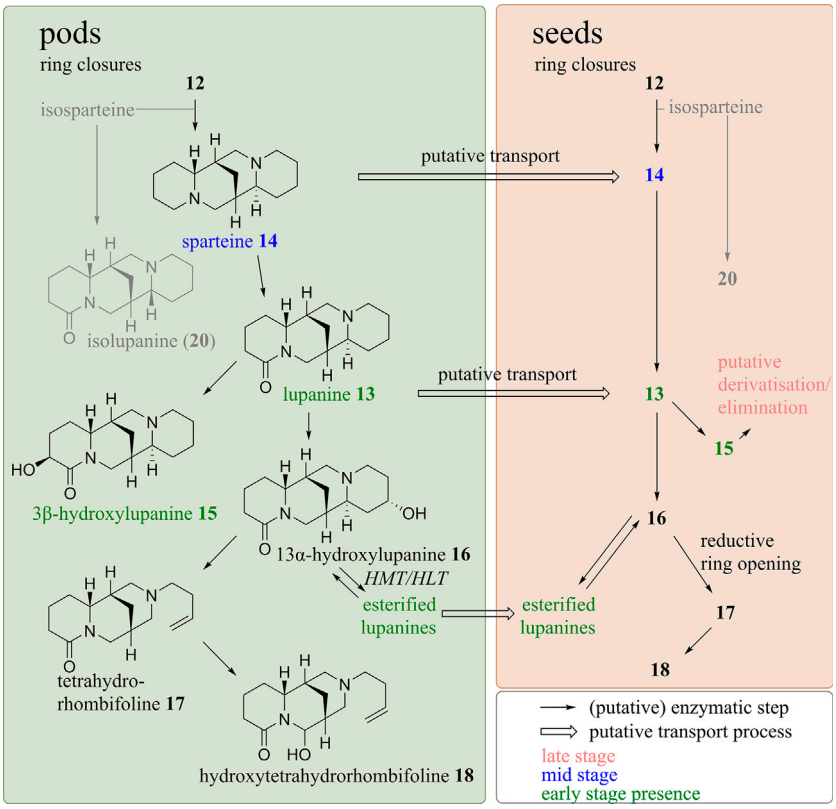


FIGURE 9
Hypothetic biosynthetic pathway interaction in *L. mutabilis*. Herein, the putative biosynthetic correlation of the major alkaloids in *L. mutabilis* is proposed according to the findings in this work. The proposed pathway hypothesis is split into pods (pale green) and seeds (beige), highlighting compounds that appear predominantly in the early stages of maturation in green, in the mid stage in blue, and in the late stage in red. The outlined arrows between pods and seeds mark putative transport entities. The transport of esterified lupanines from outside the pod-seed complex has already been proposed by Lee et al. (2006). Note that isosparteine was not observed in this study but would be the logical precursor of isolupanine (**20**). *13-hydroxylupanine O-tigloyltransferase* (HMT/HLT).

The genome-wide transcriptomics allowed a broader investigation of *L. mutabilis* homologs to known genes involved in regulating, catalyzing, and transporting QAs (see Supplementary Table S1, sheet1).

The *L. angustifolius* gene *AT* encoding an acetyltransferase was identified as the gene with a causal mutation in the *pauper* region for sweet seeds without QAs (Mancinotti et al., 2023). The identified homologs also showed stronger expression in pods than in seeds at stage 1.5, supporting the scaffold import hypothesis. The cinnamoyl-CoA reductase 2 (*CCR2*), a candidate for alkaloid biosynthesis regulation in other lupin species, followed a similar expression pattern to *LDC* and *CAO* as described before (Czepiel et al., 2021). In contrast to the scaffold hypothesis, the expression of predicted QA regulators, the *AP2/ERF* transcription factor *RAP2-7*, along with the *MYB*-family candidate *MYB106* (Kroc et al., 2019; Yang et al., 2017), being more abundant in pods, collectively indicated that both the core biosynthetic reactions and also subsequent modifications of QAs occur predominantly in pods at least in the aging stages 1.5 and 2. However, QA biosynthesis and regulator genes were expressed in the early stages in seeds to a lower amount, which might enable a smaller fraction of QA biosynthesis occurring in seeds as described in *L. albus* in earlier studies (Lee et al., 2006). Several downstream enzyme candidates, including the 13-hydroxylupanine-*O*-tigloyltransferase (*HMT/HLT*), showed presence in both organs with a surplus in the pods, which must lead to an increase in esterified lupanines (Okada et al., 2005), which are not detected in either seed or pod. Thus, the production of esterified lupanines either led to import and hydrolysis in the seeds as represented in Figure 9 or an export into other plant organs. Other pathway-related genes showed more nuanced patterns. One of the carboxylesterase 1 (*CES1L*) genes (mikado.chr2G27), involved in secondary metabolism and potentially in QA regulation, displayed its highest fold change in pods at stage 2, while mikado.chr11G658 shows reduced expression compared to the seeds. 4-Hydroxy-tetrahydrodipicolinate synthase (*DHDPS*), a key enzyme in lysine biosynthesis, showed expression patterns that do not correlate with QA levels, likely reflecting general metabolic demand for lysine rather than QA-specific regulation. Despite a decline in total QA content in pods during the development from stage 1.5 to stage 2, the sustained high expression of biosynthetic genes indicates a state of elevated metabolic turnover driven by rapid export. However, it cannot be distinguished whether all alkaloids or only scaffolds for late-stage derivatization are imported. In accordance with the literature, the seeds in *L. mutabilis*

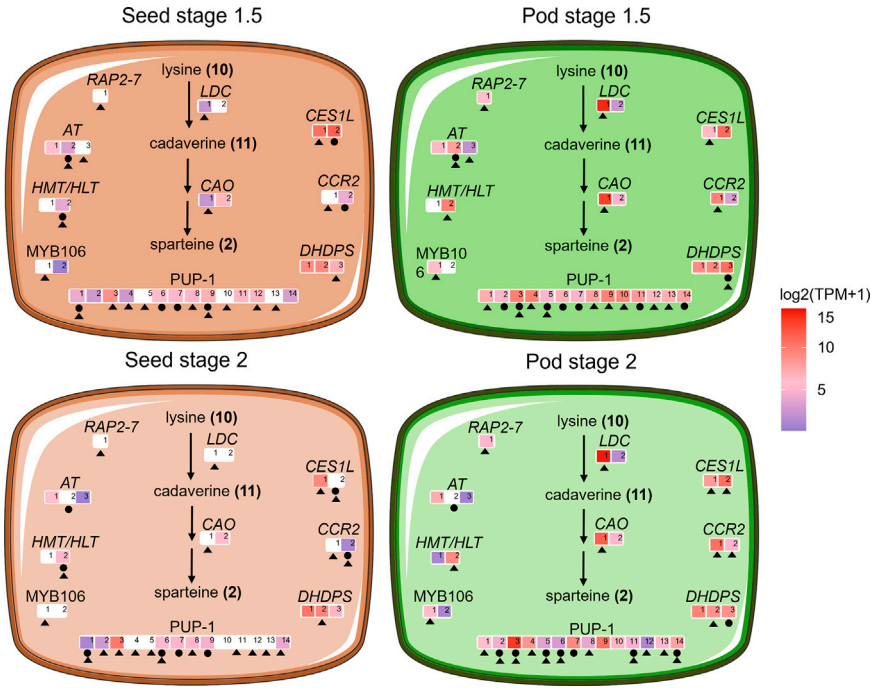


FIGURE 10
Tissue- and stage-specific expression of QA pathway genes. The figure shows expression patterns color-coded as transcripts per million (TPM) for homologous genes involved in quinolizidine alkaloid (QA) biosynthesis, transport, and regulation across different tissues and developmental stages. Significant differentially expressed genes (DEGs) based on an FDR-corrected p-value of 0.05 and $\log_2$FC $|\geq 2|$ are represented by circles indicating differences between stages and by triangles indicating differences between tissues. Genes with 0 TPM are shown as white boxes. The boxes are labeled with the numbers of homologous genes (Supplementary Table S1).

predominantly acquire QAs through transporter-mediated uptake rather than through *de novo* biosynthesis (Otterbach et al., 2019). This hypothesis is eventually supported by the expression of PUP1 transporters being enriched in pods over seeds in both stages.

5 Conclusion

This work elucidates *L. mutabilis* PI 457964 QA metabolism during seed and pod maturation. With the accumulation of valuable compounds like sparteine and lupanine, the line contains valuable compounds for putative side stream applications. The analysis showed a clear indication of a consecutive biosynthesis starting with sparteine derivatized to lupanine, which branches to multiple minor QAs. The accumulation profiles and gene expression analysis indicated that QA biosynthesis is not limited to single tissues, but rather a compilation of different import and biosynthesis processes leading to QA accumulation. The investigations into the minor alkaloids led to the finding that mostly structurally similar alkaloids accumulate and transfer at similar times. For all alkaloids, the route of transfer is from pod to seed, although the early stages of green seeds must also be biosynthetically active to perform late-stage modifications.

Data availability statement

The original contributions presented in the study are publicly available. This data can be found in the NCBI repository with the Bio project accession number: PRJNA1507228, at: https://www.ncbi.nlm.nih.gov/sra/PRJNA1507228.

Author contributions

PS: Formal analysis, Investigation, Writing – original draft, Writing – review and editing. ML: Conceptualization, Resources, Writing – original draft, Writing – review and editing. JG: Methodology, Writing – original draft, Writing – review and editing. MS: Data curation, Formal analysis, Investigation, Writing – original draft, Writing – review and editing. AB: Investigation, Writing – original draft, Writing – review and editing. AW-K: Supervision, Validation, Writing – original draft, Writing – review and editing. SB: Formal analysis, Supervision, Writing – original draft, Writing – review and editing. SN: Writing – original draft, Writing – review and editing. US: Writing – original draft, Writing – review and editing. JP: Writing – original draft, Writing – review and editing. TC: Formal analysis, Writing – original draft, Writing – review and editing.

Funding

The author(s) declared that financial support was received for this work and/or its publication. This research was funded by a grant from the Ministry of Innovation, Science, and Research within the

NRW-Strategieprojekt BioSC (No. 313/323-400-002 13) by the boost fund "P³roLucas." The authors thank Heinrich Heine University and Forschungszentrum Jülich GmbH for their generous support.

Acknowledgements

The authors gratefully acknowledge Saatzucht Steinach GmbH & Co KG for providing the bitter *L. angustifolius* line Bo9027. The language model DeepL was used for language editing. The authors would like to thank Birgit Henssen, Vera Ophoven, and Andreas Klein for their diligent support in chromatography, laboratory support, and spectroscopy.

Conflict of interest

The author(s) declared that this work was conducted in the absence of any commercial or financial relationships that could be construed as a potential conflict of interest.

The authors SB, US declared that they were an editorial board member of Frontiers at the time of submission. This had no impact on the peer review process and the final decision.

Generative AI statement

The author(s) declared that generative AI was used in the creation of this manuscript. The language model DeepL was used for language editing.

Any alternative text (alt text) provided alongside figures in this article has been generated by Frontiers with the support of artificial intelligence and reasonable efforts have been made to ensure accuracy, including review by the authors wherever possible. If you identify any issues, please contact us.

Publisher's note

All claims expressed in this article are solely those of the authors and do not necessarily represent those of their affiliated organizations, or those of the publisher, the editors and the reviewers. Any product that may be evaluated in this article, or claim that may be made by its manufacturer, is not guaranteed or endorsed by the publisher.

Supplementary material

The Supplementary Material for this article can be found online at: https://www.frontiersin.org/articles/10.3389/fntpr.2026.1797194/full#supplementary-material

References

Altschul, S. F., Gish, W., Miller, W., Myers, E. W., and Lipman, D. J. (1990). Basic local alignment search tool, *J. Mol. Biol.*, 215 (3), 403–410. doi:10.1016/S0022-2836(05)80360-2

Armbruster, D. A., and Pry, T. (2008). Limit of blank, limit of detection and limit of quantitation. *Clin. Biochem. Rev.* 29 (Suppl. 1), S49–S52.

Beier, S., Bolger, A. M., Bolger, M. E., Schwacke, R., and Usadel, B. (2026). Trimmomatic: a decade of feature-rich, high-performance NGS read preprocessing, *Bioinformatics*, 42 (6), btag331. doi:10.1093/bioinformatics/btag331

Bolger, A. M., Lohse, M., and Usadel, B. (2014). Trimmomatic: a flexible trimmer for Illumina sequence data, *Bioinformatics*, 30, 15, 2114–2120. doi:10.1093/bioinformatics/btu170

Brooke, P., Harris, D. J., and Longmore, R. B. (1996). Isolation of minor lupin alkaloids. 1. A simple procedure for the isolation of angustifoline from Lupinus angustifolius (cv. Fest) seeds, with application to other lupin alkaloids. *J. Agric. Food Chem.* 44, 2129–2133. doi:10.1021/jf950020y

Bunsupa, S., Katayama, K., Ikeura, E., Oikawa, A., Toyooka, K., Saito, K., et al. (2012). Lysine decarboxylase catalyzes the first step of quinolizidine alkaloid biosynthesis and coevolved with alkaloid production in leguminosae. *Plant Cell* 24, 1202–1216. doi:10.1105/tpc.112.095885

Byrne, P. F., Volk, G. M., Gardner, C., Gore, M. A., Simon, P. W., and Smith, S. (2018). Sustaining the future of plant breeding: the critical role of the USDA-ARS national plant germplasm system. *Crop Sci.* 58, 451–468. doi:10.2135/cropsci2017.05.0303

Cely-Veloza, W., Kato, M. J., and Coy-Barrera, E. (2023). Quinolizidine-type alkaloids: chemodiversity, occurrence, and bioactivity. *ACS Omega* 8, 27862–27893. doi:10.1021/acsomega.3c02179

Czepiel, K., Krajewski, P., Wilczura, P., Bielecka, P., Święcicki, W., and Kroc, M. (2021). Expression profiles of alkaloid-related genes across the organs of narrow-leafed lupin (Lupinus angustifolius L.) and in response to anthracnose infection. *Int. J. Mol. Sci.* 22, 2676. doi:10.3390/ijms22052676

Dracup, M., and Kirby, E. J. M. (1996). *Lupin Development Guide*. Nedlands: University of Western Australia Press.

Firn, R. D., and Jones, C. G. (2003). Natural products – a simple model to explain chemical diversity. *Nat. Product. Rep.* 20, 382–391. doi:10.1039/b208815k

Frick, K. M., Kamphuis, L. G., Siddique, K. H. M., Singh, K. B., and Foley, R. C. (2017). Quinolizidine alkaloid biosynthesis in lupins and prospects for grain quality improvement. *Front. Plant Sci.* 8, 8–2017. doi:10.3389/fpls.2017.00087

Frick, K. M., Foley, R. C., Kamphuis, L. G., Siddique, K. H. M., Garg, G., and Singh, K. B. (2018). Characterization of the genetic factors affecting quinolizidine alkaloid biosynthesis and its response to abiotic stress in narrow-leafed lupin (Lupinus angustifolius L.). *Plant, Cell and Environ.* 41, 2155–2168. doi:10.1111/pce.13172

Frick, K. M., Lorensen, M. D. B. B., Micic, N., Esteban, E., Pasha, A., Schulz, A., et al. (2025). The aerial epidermis is a major site of quinolizidine alkaloid biosynthesis in narrow-leafed lupin. *New Phytol.* 245, 2052–2068. doi:10.1111/nph.20384

Golebiewski, W. M., and Spenser, I. D. (1988). Biosynthesis of the lupine alkaloids. II. Sparteine and lupanine. *Can. J. Chem.* 66, 1734–1748. doi:10.1139/v88-280

Hama, J. R., Jorgensen, D. B. G., Diamantopoulos, E., Bucheli, T. D., Hansen, H. C. B., and Strobel, B. W. (2022). Indole and quinolizidine alkaloids from blue lupin leach to agricultural drainage water. *Sci. Total Environ.* 834, 155283. doi:10.1016/j.scitotenv.2022.155283

Hildreth, S. B., Gehman, E. A., Yang, H., Lu, R., Ritesh, K. C., Harich, K. C., et al. (2011) Tobacco nicotine uptake permease (NUP1) affects alkaloid metabolism, *Proc. Natl. Acad. Sci. U.S.A.* 108 (44) 18179–18184. doi:10.1073/pnas.1108620108

Hove, E. L. (1974). Composition and protein quality of sweet lupin seed. *J. Sci. Food Agric.* 25, 851–859. doi:10.1002/jsfa.2740250715

Kroc, M., Czepiel, K., Wilczura, P., Mokrzycka, M., and Święcicki, W. (2019). Development and validation of a gene-targeted dCAPS marker for marker-assisted selection of low-alkaloid content in seeds of narrow-leafed lupin (Lupinus angustifolius L.). *Genes*, 10 (6), 428. doi:10.3390/genes10060428

Lee, M. J., Pate, J. S., Harris, D. J., and Atkins, C. A. (2006). Synthesis, transport and accumulation of quinolizidine alkaloids in Lupinus albus L. and L. angustifolius L. *J. Exp. Bot.* 58, 935–946. doi:10.1093/jxb/erl254

Love, M. I., Huber, W., and Anders, S. (2014). Moderated estimation of fold change and dispersion for RNA-seq data with DESeq2. *Genome Biol.* 15 (12), 550. doi:10.1186/s13059-014-0550-8

Mancinotti, D., Frick, K. M., and Geu-Flores, F. (2022). Biosynthesis of quinolizidine alkaloids in lupins: mechanistic considerations and prospects for pathway elucidation. *Nat. Product. Rep.* 39, 1423–1437. doi:10.1039/d1np00069a

Mancinotti, D., Czepiel, K., Taylor, J. L., Golshadi Galehshahi, H., Møller, L. A., Jensen, M. K., et al. (2023). The causal mutation leading to sweetness in modern white lupin cultivars. *Sci. Adv.* 9, eadg8866. doi:10.1126/sciadv.adg8866

Martinez-Hernandez, J. E., Salvo-Garrido, H., Levicoy, D., Caligari, P. D. S., Rupayán, A., Moyano, T., et al. (2025). Genomic structure of yellow lupin (Lupinus luteus):

genome organization, evolution, gene family expansion, metabolites and protein synthesis. *BMC Genomics* 26, 477. doi:10.1186/s12864-025-11678-8

Muzquiz, M., Cuadrado, C., Ayet, G., DE LA Cuadra, C., Burbano, C., and Osagie, A. (1994). Variation of alkaloid components of lupin seeds in 49 genotypes of Lupinus albus from different countries and locations. *J. Agric. Food Chem.* 42, 1447–1450. doi:10.1021/jf00043a011

Namdar, D., Mulder, P. P. J., Ben-Simchon, E., Hacham, Y., Basheer, L., Cohen, O., et al. (2024). New analytical approach to quinolizidine alkaloids and their assumed biosynthesis pathways in lupin seeds. *Toxins (Basel)* 16, 163. doi:10.3390/toxins16030163

National Institute of Standards and Technology, (2023). *NIST/EPA/NIH Mass Spectral Library and Search Program (Version 2.0g) User Guide*. NIST Standard Reference Data Program.

NIST (2020). "NIST 20 tandem mass spectral library (MS/MS),". Gaithersburg, MD. *Natl. Inst. Stand. Technol. (NIST), Mass Spectrom. Data Cent.*

Okada, T., Hirai, M. Y., Suzuki, H., Yamazaki, M., and Saito, K. (2005). Molecular characterization of a novel quinolizidine alkaloid O-Tigloyltransferase: cDNA cloning, catalytic activity of recombinant protein and expression analysis in lupinus plants. *Plant Cell Physiology* 46, 233–244. doi:10.1093/pcp/pci021

Otterbach, S. L., Yang, T., Kato, L., Janfelt, C., and Geu-Flores, F. (2019). Quinolizidine alkaloids are transported to seeds of bitter narrow-leafed lupin. *J. Exp. Bot.* 70, 5799–5808. doi:10.1093/jxb/erz334

Paczia, N., Nilgen, A., Lehmann, T., Gätgens, J., Wiechert, W., and Noack, S. (2012). Extensive exometabolome analysis reveals extended overflow metabolism in various microorganisms. *Microb. Cell Factories* 11, 122. doi:10.1186/1475-2859-11-122

Patro, R., Duggal, G., Love, M. I., Irizarry, R. A., and Kingsford, C. (2017). Salmon provides fast and bias-aware quantification of transcript expression. *Nat. Methods.* 14 (4), 417–419. doi:10.1038/nmeth.4197

Plewiński, P., Książkiewicz, M., Rychel-Bielska, S., Rudy, E., and Wolko, B. (2019). Candidate domestication-related genes revealed by expression quantitative trait loci mapping of narrow-leafed lupin (Lupinus angustifolius L.). *Int. J. Mol. Sci.* 20, 5670. doi:10.3390/ijms20225670

Pueyo, J. J., Quiñones, M. A., Coba DE LA Peña, T., Fedorova, E. E., and Lucas, M. M. (2021). Nitrogen and phosphorus interplay in Lupin root nodules and cluster roots. *Front. Plant Sci.*, 12–2021. doi:10.3389/fpls.2021.644218

Rana, J., and Robins, D. J. (1984). Quinolizidine alkaloid biosynthesis: incorporation of [1-amino-15N, 1-13C]cadaverine into lupinine. *J. Chem. Soc. Chem. Commun.*, 81–82. doi:10.1039/c39840000081

Reinhard, H., Rupp, H., Sager, F., Streule, M., and Zoller, O. (2006). Quinolizidine alkaloids and phomopsins in lupin seeds and lupin containing food. *J. Chromatogr. A* 1112, 353–360. doi:10.1016/j.chroma.2005.11.079

Rodés-Bachs, C., and Van Der Fels-Klerx, H. J. (2023). Impact of environmental factors on the presence of quinolizidine alkaloids in lupins: a review. *Food Addit. Contam. Part A Chem. Anal. Control Expo. Risk Assess.* 40, 757–769. doi:10.1080/19440049.2023.2217273

Schoofs, G., Teichmann, S., Hartmann, T., and Wink, M. (1983). Lysine decarboxylase in plants and its integration in quinolizidine alkaloid biosynthesis. *Phytochemistry* 22, 65–69. doi:10.1016/s0031-9422(00)80059-x

Schrenk, D., Bodin, L., Chipman, J. K., Del Mazo, J., Grasl-Kraupp, B., Hogstrand, C., et al. (2019). EFSA Panel on Contaminants in the Food Chain: scientific opinion on the risks for animal and human health related to the presence of quinolizidine alkaloids in feed and food, in particular in lupins and lupin-derived products. *EFSA J.* 17, e05860.

Schütte, H. R., and Hindorf, H. (1965). Zur Biosynthese von Lupanin und Hydroxylupanin in Lupinus angustifolius. *Justus Liebigs Ann. Chem.* 685, 187–194. doi:10.1002/jlac.19656850124

Sievers, F., Wilm, A., Dineen, D., Gibson, T. J., Karplus, K., Li, W., et al. (2011). Fast, scalable generation of high-quality protein multiple sequence alignments using Clustal Omega. *Mol Syst Biol.* 7, 539. doi:10.1038/msb.2011.75

Talhinhas, P., Baroncelli, R., and Le Floch, G. (2016). Anthracnose of lupins caused by colletotrichum lupini: a recent disease and a successful wordwide pathogen. *J. Plant Pathology* 98, 5–14.

Van DE Noort, M. (2024). "Chapter 11 - lupin: an important protein and nutrient source," in *Sustainable Protein Sources*. S. Nadathur, J. P. D. Wanasundara, and L. Scanlin Second Edition (Academic Press).

Villalpando-Vargas, F., and Medina-Ceja, L. (2016). Sparteine as an anticonvulsant drug: evidence and possible mechanism of action. *Seizure.* 39, 49–55. doi:10.1016/j.seizure.2016.05.010

Weil, H. L., Schneider, K., Tschöpe, M., Bauer, J., Maus, O., Frey, K., et al. (2023). PLANTdataHUB: a collaborative platform for continuous FAIR data sharing in plant research. *Plant J.* 116, 974–988. doi:10.1111/tpj.16474

Wrobleski, J. T., and Long, G. J. (1977). Alkaloids as ligands. 1. Synthesis and characterization of three cobalt(II) pseudohalide compounds containing l-sparteine. *Inorg. Chem.* 16, 704–709. doi:10.1021/ic50169a041

Yang, T., Nagy, I., Mancinotti, D., Otterbach, S. L., Andersen, T. B., Motawia, M. S., et al. (2017). Transcript profiling of a bitter variety of narrow-leafed lupin to discover alkaloid biosynthetic genes. *J. Exp. Bot.* 68, 5527–5537. doi:10.1093/jxb/erx362

Zeng, F., Yan, Y., Chen, C., Liu, L., Li, B., Li, Y., et al. (2025). New avenues for asymmetric synthesis: N–H (+)-sparteine and analogues. *Green Synthesis Catal.* doi:10.1016/j.gresc.2025.06.005